

# $^{77}\text{Se}$ NMR Investigation of Fe-doped $\text{Bi}_2\text{Se}_3$

Robert E. Taylor<sup>†</sup>, Hamad M. Alyahyaei<sup>#</sup>, Zhiyong Wang<sup>#</sup>, Jing Shi<sup>#</sup>, Mark A. Zurbuchen<sup>&</sup>,  
Belinda Leung<sup>†</sup>, Nanette N. Jarenwattananon<sup>†</sup>, Xufeng Kou<sup>\*</sup> and Louis-S Bouchard<sup>1†§</sup>

<sup>†</sup>Department of Chemistry and Biochemistry, <sup>&</sup>Electrical Engineering Department, Western Institute for Nanoelectronics, <sup>§</sup>California NanoSystems Institute, University of California, Los Angeles, CA 90095, USA.

<sup>#</sup>Department of Physics, University of California, Riverside, CA 92521, USA. <sup>\*</sup>Department of Electrical Engineering, University of California, Los Angeles, CA 90095, USA

Bismuth selenide is both a thermoelectric material and topological insulator. Defects and dopants create conduction in thermoelectric applications. However, such defects may degrade the performance as a topological insulator (TI). Magnetic impurities such as iron open a band gap at the Dirac point on the surface. Since magnetically-doped TIs are important in technological applications, a good understanding of their properties is needed. In this article,  $^{77}\text{Se}$  nuclear magnetic resonance (NMR) spectroscopy has been used to investigate Fe-doped  $\text{Bi}_2\text{Se}_3$ . Spin-lattice relaxation measurements indicate that the Fe dopants provide a spin diffusion relaxation mechanism at low temperatures for the  $^{77}\text{Se}$ . Above 320 K, the predominant  $^{77}\text{Se}$  relaxation mechanism resulting from interaction with the conduction carriers is thermally induced with an activation energy of 21.5 kJ/mol (5.1 kcal/mol, 222 meV) and likely arises from inter-band excitations. Magic-angle spinning produces negligible narrowing of the  $^{77}\text{Se}$  resonance at 7 T, suggesting a statistical distribution of material defects and is also consistent with a dipolar interaction with the neighboring quadrupolar nucleus.

---

<sup>1</sup> Corresponding author: [bouchard@chem.ucla.edu](mailto:bouchard@chem.ucla.edu)

## I. INTRODUCTION

The thermoelectric (TE) properties of bismuth chalcogenides have long been known. In particular, bismuth selenide ( $\text{Bi}_2\text{Se}_3$ ) has been “considered as a model compound among thermoelectric materials for both experimental and theoretical analysis”<sup>1</sup>. While bismuth telluride is the most commonly used thermoelectric material, the scarcity of Te is leading to a search for alternatives<sup>2</sup> and improvements in other thermoelectric materials such as  $\text{Bi}_2\text{Se}_3$ <sup>3-5</sup>.

Bismuth selenide is also a topological insulator (TI)<sup>6-7</sup>. The novel electromagnetic properties of the surfaces of these materials are receiving much attention in condensed-matter physics<sup>8</sup>. These materials typically have insulating band gaps in the bulk with a gapless surface state protected by time-reversal symmetry (TRS). However, magnetic impurities such as Cr, Fe or Mn break the TRS and open a gap at the Dirac point<sup>8</sup>. The strong interest in magnetically doped TIs stems from their fundamental role in experimental realizations of the topological magneto-electric effect<sup>9-10</sup>, Kerr and Faraday effects<sup>11-12</sup>, spin transfer<sup>13</sup>, anomalous magnetoresistance<sup>14</sup>, and the anomalous Hall effect (AHE)<sup>15-18</sup>.

In this work, we have investigated structural and nuclear-magnetic properties of Fe-doped  $\text{Bi}_2\text{Se}_3$ , with the aim of gaining a better understanding of the role of dopants in the lattice. Such investigations are much-needed because the quality and the utility of TI and TE samples are related to the presence of dopants, impurities and lattice defects. The nuclear magnetic resonance (NMR) technique provides a better understanding of the defects leading to suboptimal insulating properties by enabling investigation of mechanisms that lead to conduction. Specifically, NMR can probe the coupling of specific lattice site nuclei to the conduction band charge carriers. Such site-specific measurements can be used to probe the involvement of local

orbitals in the conduction process. Our recent study<sup>19</sup> of  $\text{Bi}_2\text{Se}_3$  and  $\text{Bi}_2\text{Te}_3$  has shown the role that spin-orbit coupling plays in the nuclear relaxation. This current work extends the investigation to iron-doped bismuth selenide.

## II. EXPERIMENTAL METHODS

### A. Sample Preparation

Single crystals of  $\text{Fe}_x\text{Bi}_2\text{Se}_3$  were grown using a multi-step heating method described elsewhere<sup>20</sup>. First, high-purity (99.999%) Bi and high purity (99.998%) Fe were mixed in a ratio of 95:5 according to mass and sealed in an evacuated quartz tube. The tube was then heated to and held at 1373 K for 24 hours in a programmable furnace. It was subsequently cooled to and held at 773 K for 72 hours before it was finally cooled to room temperature. Although higher iron-content samples clearly show room temperature ferromagnetism, for the present sample there is only a small magnetic hysteresis with a saturation magnetic moment less than 1% of the total iron moments, indicating that a vast majority of the iron are in the paramagnetic state at room temperature. Fig. 1(a) depicts the magnetic hysteresis at 4 K. Transport measurements, shown in Fig. 1(b), indicate that the Fermi level lies in the conduction band.

The solid-state synthesis reaction yielded  $\text{Fe}_x\text{Bi}_2\text{Se}_3$  ( $x = 0.02$ ) as shown by powder x-ray diffraction (PXRD) and inductively-coupled plasma optical emission spectroscopy (ICP-OES) analysis. The details of this analysis, which will be published elsewhere<sup>21</sup>, are consistent with iron substituting on the Se(1) site whereas the final molar ratio was determined to be: Bi = 2.000, Se = 2.908 and Fe = 0.022. In the text below, this sample will be denoted as  $\text{Fe}_x\text{Bi}_2\text{Se}_3$ ,  $x = 0.02$  or simply  $\text{Fe}_x\text{Bi}_2\text{Se}_3$ . This interpretation differs from published literature which has classified the Fe dopant as a substituent to the Bi site<sup>22-23</sup> or as an interstitial dopant<sup>24</sup>.

The analysis of PXRD data also indicated<sup>21</sup> that the material forms a single phase, where the doping level used ( $x = 0.02$ , or 5.1 %) was below the solubility limit (10-20%) of Fe in  $\text{Bi}_2\text{Se}_3$ .

## B. <sup>77</sup>Se NMR Characterization

The <sup>77</sup>Se NMR data were acquired with a Bruker DSX-300 spectrometer operating at a frequency of 57.30 MHz with a static sample using a standard Bruker X-nucleus wideline probe with a 5-mm solenoid coil. The  $\text{Fe}_x\text{Bi}_2\text{Se}_3$  crystals were ground with NaCl to prevent inter-particle contact of the  $\text{Fe}_x\text{Bi}_2\text{Se}_3$  and thus avoid radio frequency (RF) skin-depth issues. A ratio of NaCl to  $\text{Fe}_x\text{Bi}_2\text{Se}_3$  of about 50 weight % was used. The sample was confined to the length of the RF coil, and the <sup>77</sup>Se  $\pi/2$  pulse width was 4  $\mu\text{s}$ . We have verified that this pulse was of sufficiently wide bandwidth to cover the entire NMR spectrum where signal exists. The center frequency of the RF pulse was varied (along with probe retuning) to ensure that all resonances were captured and that the spectrum was not distorted as a result of probe tuning. Magic-angle spinning (MAS) data were acquired on the same sample with a standard Bruker MAS probe using a 4-mm outside diameter zirconia rotor. The <sup>77</sup>Se  $\pi/2$  pulse width was 4.4  $\mu\text{s}$ .

Spectral data were acquired using a spin-echo sequence  $[\pi/2]_x - \tau - \pi_y - \tau - \text{acquire}]$ . The echo delay,  $\tau$ , was set to 10  $\mu\text{s}$ . The spin-echo sequence is useful for minimizing pulse ringdown effects and for the recovery of the chemical shielding interaction in the presence of heteronuclear dipolar coupling. Simulation of the chemical-shift powder pattern for the spectrum obtained from the static sample was performed with the solids simulation package (“solaguide”) in the TopSpin (Version 3.0) NMR software program from Bruker BioSpin.

Data for determining the <sup>77</sup>Se spin-lattice relaxation ( $T_1$ ) were acquired with a saturation-recovery technique<sup>24</sup>. Temperature measurements were calibrated with the <sup>207</sup>Pb chemical shift

of lead nitrate<sup>25</sup>. The <sup>77</sup>Se chemical shift scale was calibrated using the unified  $\Xi$  scale<sup>26</sup>, relating the <sup>77</sup>Se shift to the <sup>1</sup>H resonance of dilute tetramethylsilane in CDCl<sub>3</sub> at a frequency of 300.13 MHz.

### III. RESULTS AND DISCUSSION

Bi<sub>2</sub>Se<sub>3</sub> crystallizes in the rhombohedral space group  $D_{3d}^5 (R\bar{3}m)$  with three formula units per unit cell<sup>6</sup>. This ABC-type structure consists of five atomic layers forming a quintuple layer with the order Se(2)-Bi-Se(1)-Bi-Se(2), layered along  $c$ . Bonding is strong between atomic layers within the quintuple layer, while the quintuple layers are bound by weaker van der Waals' interactions. This structure gives rise to two different selenium sites, one bonded to Bi atoms with the second on the quintuple layer edge with the van der Waals' interaction with Se in another quintuple layer. The most common defect in Bi<sub>2</sub>Se<sub>3</sub> arises from selenium vacancies<sup>27</sup>. The results from sample analysis (PXRD and ICP-OES) indicate that the iron dopant substitutes for Se(1).

Most elemental and binary semiconductors crystallize with cubic symmetry<sup>28</sup>. The high symmetry found in these materials is usually apparent in the NMR spectra. However, the  $D_{3d}^5 (R\bar{3}m)$  space group for the Bi<sub>2</sub>Se<sub>3</sub> has lower symmetry which can lead to more complicated spectra. The absence of cubic symmetry can give rise to anisotropy in the chemical shift<sup>29-30</sup> and Knight shift<sup>31</sup>. More than one spectral resonance may arise from the two crystallographically distinct sites for Se in the quintuple layers of Bi<sub>2</sub>Se<sub>3</sub> lattice. In addition, an inhomogeneous distribution of defects can give rise to a distribution of Knight shifts resulting from the dependence of the Knight shift upon the charge carrier concentration<sup>32,33</sup>. The analysis of the resonant lineshape is challenging due to this high number of nuclear interactions. As MAS<sup>34-36</sup> does not distinguish between these interactions in the sample studied here (*vide infra*), the same

technique of using a single tensorial interaction to simulate the lineshapes in semiconducting samples<sup>19,37</sup>, rather than trying to separate the chemical and Knight shift contributions, has been used in the analysis presented here. This approach provides a quantitative framework for the description and comparison of the <sup>77</sup>Se resonance in this material to those investigated previously<sup>19</sup>.

The <sup>77</sup>Se wideline NMR spectrum of Fe<sub>x</sub>:Bi<sub>2</sub>Se<sub>3</sub> acquired with a spin-echo technique is shown in Fig. 2(a). The thin green line in Fig. 2(a) is the result of a simulation to determine the principal components of the NMR shift tensor. The extracted parameters of this interaction are given in Table I. These spectral parameters are quite similar to those previously reported for Bi<sub>2</sub>Se<sub>3</sub><sup>19</sup>. This line shape likely indicates a distribution of material defects or charge carrier domains, both of which can cause the broadening observed. The anisotropy of the powder pattern observed is consistent with the material anisotropy and the absence of cubic symmetry<sup>29-31</sup>.

The powder <sup>77</sup>Se NMR pattern was independent of temperature over the range studied (Fig. 2(b)), suggesting that coupling to the conduction band and diamagnetism dominate over paramagnetic effects in this heavily doped sample. This does not, however, mean that paramagnetism is absent. On the contrary, the SQuID results (Fig. 1(a)) suggest strong paramagnetism. Instead, these NMR results indicate that nuclei which are located close to the paramagnetic iron centers are likely broadened to the point of being undetectable by NMR (*vide infra*).

MAS<sup>34-36</sup>, normally used to narrow the spectral lines in NMR, does not significantly narrow the <sup>77</sup>Se resonance (Fig. 3) at the modest field used in this study (7 T). There are four possible contributions to this MAS result. One is that the dipolar coupling of the quadrupolar

$^{209}\text{Bi}$  (Table II) to the spin- $1/2$   $^{77}\text{Se}$  is not averaged to zero<sup>38-43</sup>. At this magnetic field strength of 7 T, the electric quadrupole interaction<sup>26</sup> for the  $^{209}\text{Bi}$  may be comparable to the Zeeman interaction and can result in a mixing of the pure Zeeman states. Residual terms in the resulting dipolar Hamiltonian are larger (in frequency units) than the rate of MAS. We note that because this effect can be described with higher-order perturbation theory where dipolar and quadrupolar couplings are mixed, the broadening resulting from this effect can be much larger than the magnitude of the dipole-dipole coupling itself, which is at most a few hundred Hertz for this sample. This same effect has been demonstrated with the spin- $1/2$   $^{199}\text{Hg}$  MAS spectra of the semiconducting mercuric halides<sup>43</sup> at this same 7 T magnetic field. While the  $^{35,37}\text{Cl}$  quadrupolar moments<sup>26</sup> at  $-6.78 \text{ fm}^2$  and  $-8.165 \text{ fm}^2$  are small enough that a  $^{199}\text{Hg}$  MAS spectrum of  $\text{HgCl}_2$  yields narrow resonances to which a Herzfeld–Berger<sup>44</sup> simulation can be applied to extract the principal values of the chemical shift tensor, this method of analysis was shown to produce negligible line narrowing for both  $\text{HgBr}_2$  and  $\text{HgI}_2$  as the size of the quadrupolar coupling constant of the halide becomes larger. The quadrupolar moment for  $^{209}\text{Bi}$  at  $-51.6 \text{ fm}^2$  is between that of  $^{79}\text{Br}$  ( $31.3 \text{ fm}^2$ )<sup>26</sup> and  $^{127}\text{I}$  ( $-71.0 \text{ fm}^2$ )<sup>26</sup>. Symmetry is unlikely to play a role in reducing the magnitude of the quadrupolar interaction as the linear bonding in the mercuric halides is similar to the linear bonding in the Se-Bi-Se-Bi-Se units. Acquisition of  $^{77}\text{Se}$  MAS spectra at a higher magnetic field strength could indicate whether this explanation is correct or not. However, access to higher field solid-state NMR spectrometers was not immediately available for the present study.

A second possibility could result from disorder in the sample. This situation has been reported for  $^{77}\text{Se}$  spectral resonances in glasses in which the  $^{77}\text{Se}$  is adjacent to other quadrupolar nuclei such as  $^{121,123}\text{Sb}$  and  $^{75}\text{As}$  in  $\text{Sb}_2\text{Te}_3$ <sup>45</sup>, and  $\text{As}_x\text{Se}_{(1-x)}$ <sup>46</sup>. These articles did not address

whether spectral broadening of the  $^{77}\text{Se}$  resonance might have some contribution from being adjacent to quadrupolar nuclei with sizable quadrupolar coupling constants. Nevertheless an argument against this explanation of MAS failing to narrow the resonance as a result of structural disorder in the current sample is the high crystallinity indicated by the PXRD results shown in Fig. 4.

A third source of spectral broadening of the  $^{77}\text{Se}$  MAS resonance could result from interaction with the dilute paramagnetic iron dopants. However, Abragam<sup>47</sup> has noted that “the instantaneous electronic field is smaller than the nuclear local field for all nuclei except a small minority of those abnormally close to the paramagnetic impurity.” For those nuclei “abnormally close” to the paramagnetic iron (the “wipeout sphere”), the spectral resonances can be shifted and broadened beyond observation. NMR signals from nuclei outside of this “wipeout sphere” will still be observed. As a specific example for this type of situation, MAS has been shown to narrow the  $^{31}\text{P}$  resonances (and has shown patterns of spinning sidebands) when paramagnetic species such as  $\text{Fe}^{3+}$ ,  $\text{Mn}^{2+}$  and  $\text{Cu}^{2+}$  at similar concentrations to that of iron in the current bismuth selenide sample were substituted for calcium in hydroxyapatites<sup>48</sup>. As MAS is known to narrow the spectral resonances in samples containing paramagnetic species, this interaction is not likely to be the reason for the lack of resonance narrowing in the iron-doped bismuth selenide. The more important interaction of these paramagnetic centers is the effect upon the spin-lattice relaxation of the nuclear spin system (*vide infra*).

A final possibility may be due to an interaction(s) with the conduction charge carriers in this material. This lack of narrowing of the spectral resonance by MAS led to a new investigation of semiconducting lead telluride. All the NMR-active nuclei in lead telluride are spin- $\frac{1}{2}$ . Yet neither the  $^{207}\text{Pb}$  nor the  $^{125}\text{Te}$  spectral resonances were significantly narrowed by

MAS<sup>49</sup>. This result suggests an interaction with the conduction charge carriers or an inhomogeneity in the distribution of charge carriers. Interaction with quadrupolar nuclei may not be the cause of MAS narrowing the resonances, as lead telluride has no quadrupolar nuclei. Regardless of the explanation, MAS at the magnetic field strength used in this study could not resolve the two <sup>77</sup>Se sites in the material. As the resonances do not break into sidebands upon MAS, the spectral broadening observed in the iron-doped bismuth selenide is not inhomogeneous. The resonance lineshape cannot be due to a simple distribution of NMR shifts (chemical shifts or Knight shifts) resulting from an orientational dependence.

The modified Carr-Purcell-Meiboom-Gill (CPMG) sequence, which has been applied to solid-state spectra of quadrupolar nuclei<sup>50</sup> as well as to spin-1/2 nuclei having large chemical shift anisotropies<sup>51-52</sup>, is another method typically used to improve sensitivity. The relatively short spin-spin relaxation time under the CPMG sequence of  $T_2^{\text{CPMG}} \sim 600 \mu\text{s}$  measured at 295 K provides little sensitivity enhancement for  $\text{Fe}_x\text{Bi}_2\text{Se}_3$ , as shown in Fig. 3. The combination of a single spin echo with MAS resulted in a significant loss of sensitivity (Fig. 3). The CPMG result may indicate that the neighboring <sup>209</sup>Bi nuclei play a role in enhancing the effects of the dipole-dipole interaction.

<sup>77</sup>Se saturation-recovery spin-lattice relaxation ( $T_1$ ) data were acquired as a function of temperature. Figure 5 shows a plot of the natural logarithm of the <sup>77</sup>Se  $T_1$  plotted as a function of the inverse of temperature. Two distinct relaxation mechanisms are apparent. At temperatures of 320 K and below, the spin-lattice relaxation is independent of temperature. This is consistent with relaxation by the paramagnetic iron dopants occurring through spin diffusion<sup>47</sup>. Above 320 K, the laboratory-frame relaxation data indicate a thermally activated relaxation mechanism.

The temperature dependence of the relaxation time assumes a correlation time that is thermally activated:

$$\tau_c(T) = \tau_0 \exp \left[ \frac{E_a}{RT} \right], \quad (1)$$

where  $\tau_0$  specifies the magnitude of the correlation time, and  $E_a$  is an activation energy for the process that modulates the dipole-dipole interaction between nearby spins. The slope of Fig. 5 yields an activation energy for this process of 21.5 kJ/mol (5.1 kcal/mol, 222 meV). The cause for this thermally activated relaxation process is consistent with inter-band excitations of the conduction band charge carriers.

Transport measurements (Fig. 1(b)) confirm that the sample is electrically conductive. For conductors, the nuclear spin-lattice relaxation is usually dominated by interaction with the conduction band electrons. Our previous study<sup>19</sup> has shown that this interaction occurs through a spin-orbit coupling for Bi<sub>2</sub>Se<sub>3</sub>, yielding a very short <sup>77</sup>Se  $T_1$  of 0.63 s. Electronic structure calculations<sup>53</sup> for the conduction band electrons in Bi<sub>2</sub>Se<sub>3</sub> show that *s*-band electrons are only a negligible fraction of the electron density of states across the conduction band. As no hyperfine contact term arises, this leaves spin-orbit coupling as the predominant interaction.

The <sup>77</sup>Se  $T_1$  of the stoichiometric Bi<sub>2</sub>Se<sub>3</sub> insulator phase is greater than 60 seconds<sup>19</sup>. The absence of observation of either an exponential saturation recovery or a biexponential saturation recovery with a short <sup>77</sup>Se  $T_1$  on the order of 0.6 s is explained by the iron doping. In our samples, any <sup>77</sup>Se nuclei in the vicinity of iron dopant, a defect creating a charge carrier that interacts with the conduction charge carrier likely has its resonance broadened beyond observation, due to the interaction with the paramagnetic iron atom. At 320 K and below, relaxation of the rest of the <sup>77</sup>Se nuclei occurs through spin diffusion with the paramagnetic iron dopants. What is important is that no evidence of a very long <sup>77</sup>Se  $T_1$  of greater than 30 s arising

from the  $\text{Bi}_2\text{Se}_3$  insulator is observed. Above 320 K, the thermal mobility of the conduction charge carriers provides the dominant relaxation mechanism. This shows the whole sample to be a semiconductor as opposed to consisting of domains of both semiconducting and insulating  $\text{Bi}_2\text{Se}_3$ ; a scenario observed in commercially available  $\text{Bi}_2\text{Se}_3$  from chemical supplier Alfa Aesar<sup>19</sup>.

#### IV. CONCLUSION

Crystalline powders of  $\text{Fe}_x\text{Bi}_2\text{Se}_3$  were studied by  $^{77}\text{Se}$  NMR spectroscopy. The principal components of the  $^{77}\text{Se}$  shift tensor exhibited substantial anisotropy, indicating a strong ordering of the orbital currents in the crystal lattice in response to an externally applied magnetic field. The paramagnetic Fe provides the dominant relaxation mechanism for  $^{77}\text{Se}$  below 320 K, while a thermally activated mechanism arising from the conduction charge carriers provides the dominant relaxation mechanism at temperatures above 320 K. The activation energy for this process is 21.5 kJ/mol (5.1 kcal/mol, 222 meV). MAS did not significantly narrow the  $^{77}\text{Se}$  resonance at a magnetic field of 7 T, which could be due to interaction with conduction charge carriers in the presence of material defects or modulation of the dipole-dipole interaction to the neighboring quadrupolar  $^{209}\text{Bi}$ . The short spin-spin relaxation time under the CPMG sequence of  $T_2^{\text{CPMG}} \sim 600 \mu\text{s}$  at ambient temperature may indicate that the neighboring  $^{209}\text{Bi}$  nuclei play a role in enhancing the effects of the dipole-dipole interaction.

## **ACKNOWLEDGMENTS**

The work at UCR was supported in part by FENA/FCRP. The work at UCLA was supported by DARPA. L.-S. B. acknowledges useful discussions with M.G. Kanatzidis, S.D. Mahanti, Faxian Xiu and Yabin Fan.

## TABLES

Experiment	$\delta_{11}$	$\delta_{22}$	$\delta_{33}$	$\delta_{\text{iso}}$	$\zeta_{\text{csa}}^{\text{a}}$	$\eta^{\text{b}}$	$\Omega^{\text{c}}$	$\kappa^{\text{d}}$
Static <sup>e</sup>	296	190	-340	49.0	-389	0.272	636	0.67

<sup>a</sup> $\zeta_{\text{csa}} = \delta_{33} - \delta_{\text{iso}}$ .  
<sup>b</sup> $\eta = (\delta_{22} - \delta_{11})/\zeta_{\text{csa}}$ .  
<sup>c</sup> $\Omega = |\delta_{33} - \delta_{11}|$ .  
<sup>d</sup> $\kappa = 3(\delta_{22} - \delta_{\text{iso}})/\Omega$ .  
<sup>e</sup>Chemical shifts are in part per million (ppm) and referenced using the  $\Xi$  scale, relating the  $^{77}\text{Se}$  shift to the  $^1\text{H}$  resonance of dilute tetramethylsilane in  $\text{CDCl}_3$  at a frequency of 300.13 MHz. (Ref. [26]).

Isotope	Spin	Natural Abundance (%)	Magnetogyric Ratio ( $\gamma/10^7 \text{ rad s}^{-1} \text{ T}^{-1}$ )	Quadrupolar Moment ( $Q/\text{fm}^2$ )
$^{57}\text{Fe}$	1/2	2.119	0.8680624	--
$^{77}\text{Se}$	1/2	7.63	5.1253857	--
$^{209}\text{Bi}$	9/2	100	4.3750	-51.6

<sup>a</sup>From Ref. [26]

## FIGURES AND FIGURE CAPTIONS

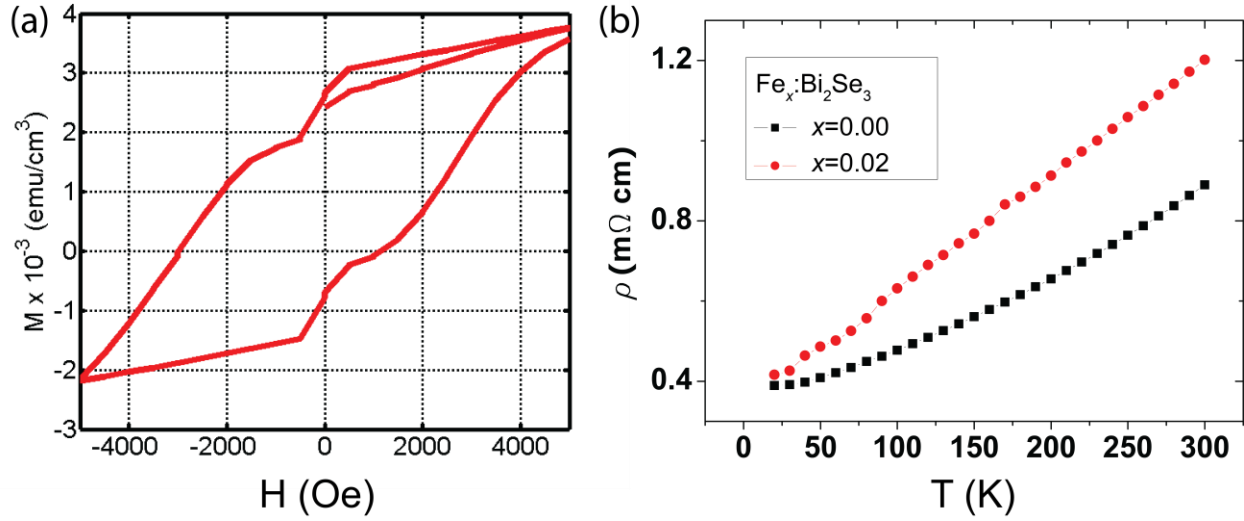


**FIG 1.** (Color online) Magnetic and electrical characterization of the  $\text{Fe}_x\text{:Bi}_2\text{Se}_3$  samples.

(a) Magnetic hysteresis curve for  $x = 0.02$  at 4 K acquired with a SQUID susceptometer reveals ferromagnetism. (b) Transport measurements for  $x = 0.00$  and  $x = 0.02$  indicate the materials behave like conductors.

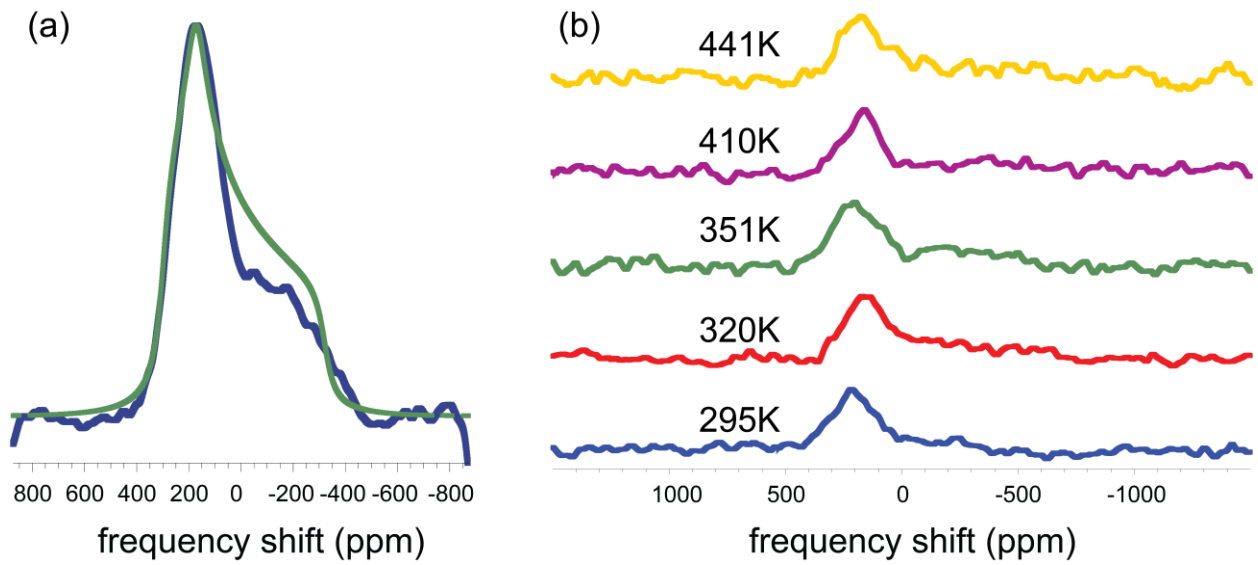


**FIG 2.** (Color online)  $^{77}\text{Se}$  NMR shift spectra. (a)  $^{77}\text{Se}$  wideline NMR spectrum (blue) of  $\text{Fe}_x\text{:Bi}_2\text{Se}_3$ . The smooth line (green) is a simulation to extract the principal components of the shift tensor. (b) The  $^{77}\text{Se}$  NMR shift is independent of temperature.

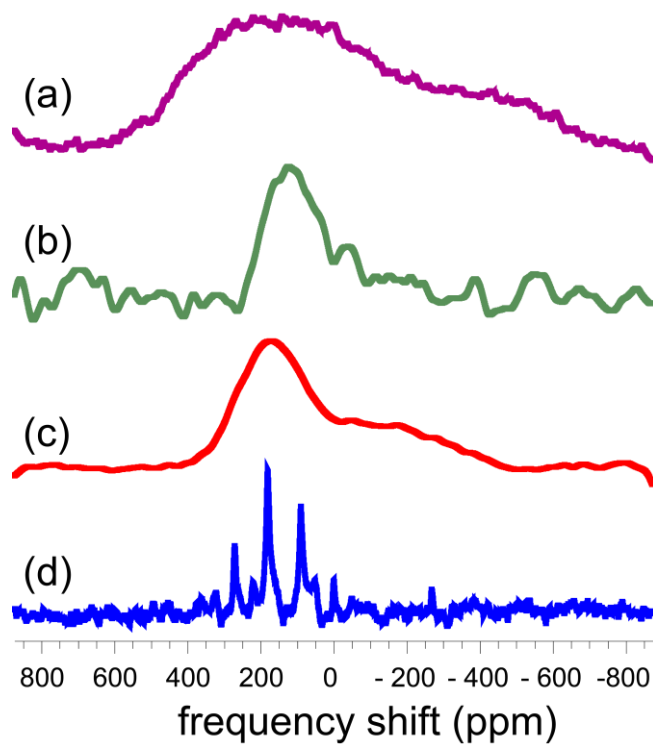


**FIG 3.** (Color online)  $^{77}\text{Se}$  NMR spectra acquired with (a) a single pulse and MAS at a spin rate of 10 kHz (top, in purple), (b) a spin echo with MAS at a spin rate of 10 kHz (in green), (c) a spin echo with a static sample (in red), and (d) a modified Carr-Purcell-Meiboom-Gill sequence with a static sample (bottom, in blue).

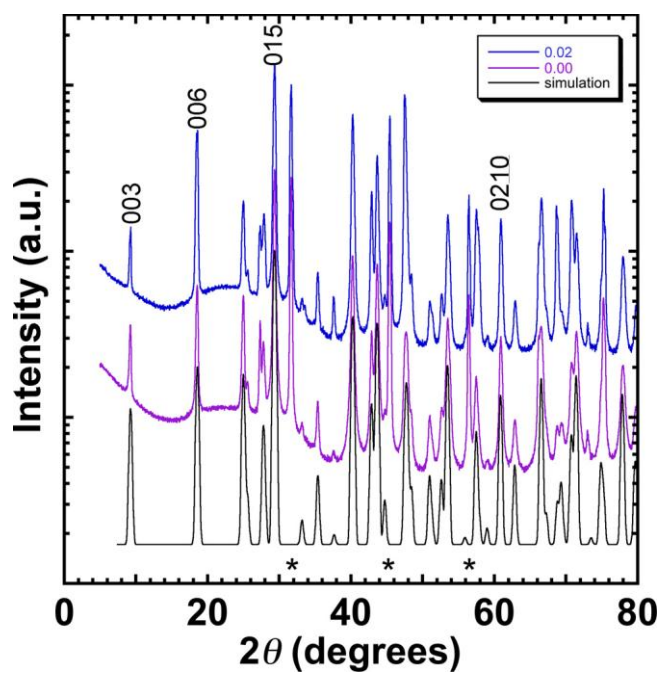


**FIG 4.** (Color online)  $\theta$ - $2\theta$  XRD scans of  $\text{Fe}_x\cdot\text{Bi}_2\text{Se}_3$  samples, for  $x=0.00$  and  $0.02$ , as indicated in the legend. A simulation of pure  $\text{Bi}_2\text{Se}_3$  is shown at the bottom for comparison. The Miller indices of the two pairs of coplanar  $\text{Bi}_2\text{Se}_3$  peaks useful for comparing relative stoichiometry are labeled. \*'s indicate NaCl peaks (added for NMR analysis). Log scale.

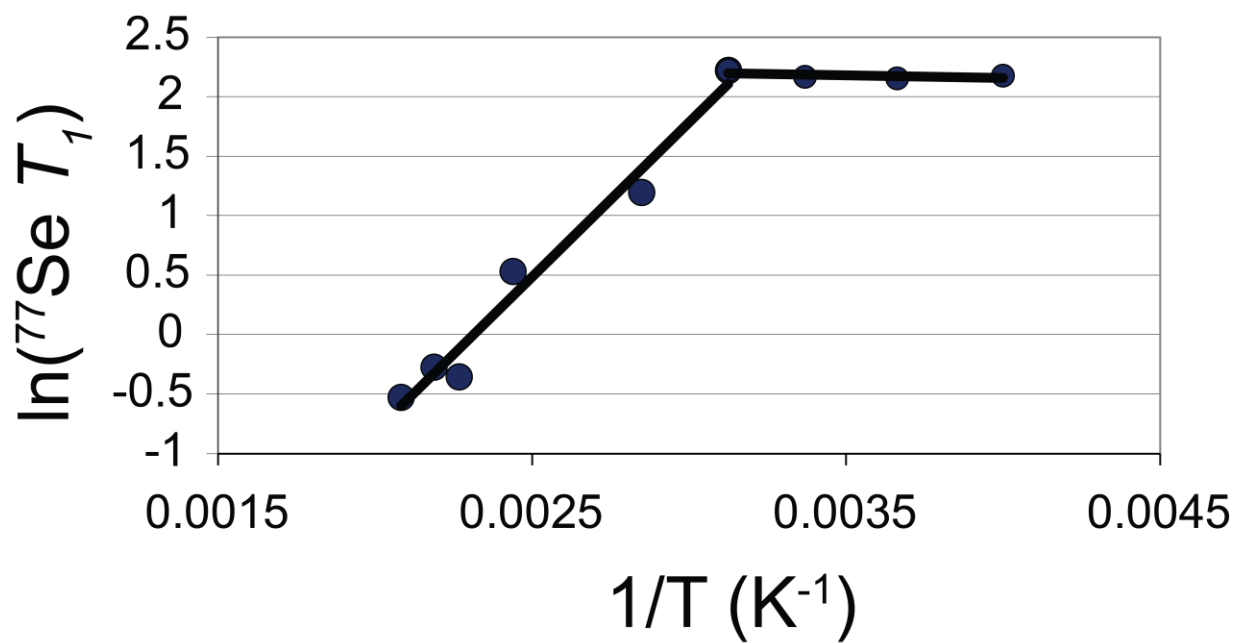


**FIG 5.** The natural logarithm of the  $^{77}\text{Se } T_1$  plotted as a function of inverse temperature.

## REFERENCES

- <sup>1</sup>A. Saji, S. Ampili, S-H. Yang, K.J. Ku, and M. Elizabeth, *J. Phys.: Condens. Matter* **17** (2005) 2873-2888.
- <sup>2</sup>D. Parker and D. J. Singh, *Phys. Rev. X* **1**, 021005 (2011).
- <sup>3</sup>K. Kadel, L. Kumari, W-Z. Li, J. Y. Huang, and P. P. Provencio, *Nanoscale Res. Lett.* **6** (2011) 57.
- <sup>4</sup>R. K. Ramesh, G. Kedarnath, V. K. Jain, A. Wadawale, M. Nalliath, C. G. S. Pillai and B. Vishwanadh, *Dalton Trans.*, **39** (2010) 8779–8787.
- <sup>5</sup>O. C. Monteiro, T. Trindade, F. A. Almeida Paz, J. Klinowski, J. Waters and P. O'Brien, *J. Mater. Chem.*, **13** (2003) 3006–3010.
- <sup>6</sup>H. Zhang, C-X. Liu, X-L. Qi, X. Dai, Z. Fang and S-C. Zhang, *Nature Physics* **5** (2009) 438-442.
- <sup>7</sup>Y. Xia, D. Qian, D. Hsieh, L. Wray, A. Pal, H. Lin, A. Bansil, D. Grauer, Y. S. Hor, R. J. Cava and M. Z. Hasan, *Nature Physics* **5** (2009) 398.
- <sup>8</sup>M. Z. Hasan and C. L. Kane, *Rev. Modern Phys.* **82** (2010) 3045-3067.
- <sup>9</sup>Qi, X.-L., T. Hughes, and S.-C. Zhang, 2008b, *Phys. Rev. B* **78**, 195424.
- <sup>10</sup>Qi, X.-L., R. Li, J. Zang, and S.-C. Zhang, 2009, *Science* **323**, 1184
- <sup>11</sup>W.-K. Tse and A. H. MacDonald, *Phys. Rev. Lett.* **105**, 057401 (2010)
- <sup>12</sup>W.-K. Tse and A. H. MacDonald, *Phys. Rev. B* **82**, 161104 (2010)
- <sup>13</sup>K. Nomura and N. Nagaosa, *Phys. Rev. B* **82**, 161401 (2010)
- <sup>14</sup>T. Yokoyama, Y. Tanaka, and N. Nagaosa, Anomalous magnetoresistance of a two-dimensional ferromagnet/ferromagnet junction on the surface of a topological insulator, *Phys. Rev. B* **81**, 121401 (2010)
- <sup>15</sup>R. Yu, W. Zhang, H. J. Zhang, S.-C. Zhang, X. Dai, and Z. Fang, Quantized anomalous Hall effect in magnetic topological insulators. *Science* **329**, 61-64 (2010)
- <sup>16</sup>Qi, X.L., Wu, Y.S. & Zhang, S.-C. Topological quantization of the spin Hall effect in two-dimensional paramagnetic semiconductors. *Phys. Rev. B* **74**, 045125 (2006)
- <sup>17</sup>Liu, C.-X., Qi, X.-L., Dai, X., Fang, Z. & Zhang, S.-C. Quantum anomalous Hall effect in Hg<sub>1-y</sub>Mn<sub>y</sub>Te quantum wells. *Phys. Rev. Lett.* **101**, 146802 (2008)
- <sup>18</sup>Qi, X.-L., Hughes, T. L. & Zhang, S.-C. Topological field theory of time-reversal invariant insulators. *Phys. Rev. B* **78**, 195424–43 (2008)
- <sup>19</sup>R. E. Taylor, B. Leung, M. P. Lake, and L-S. Bouchard, submitted.

- <sup>20</sup>Z. Wang, T. Lin, P. Wei, X. Liu, R. Dumas, K. Liu, and J. Shi, *Appl. Phys. Lett.* **97** (2010) 042112.
- <sup>21</sup>M. A. Zurbuchen, H. Alyahyaei, B. Leung, J. Shi, L.-S. Bouchard, submitted.
- <sup>22</sup>Hsieh, D. et al. Observation of time-reversal-protected single-Dirac-cone topological-insulator states in Bi<sub>2</sub>Te<sub>3</sub> and Sb<sub>2</sub>Te<sub>3</sub>. *Phys. Rev. Lett.* **103**, 146401 (2009)
- <sup>23</sup>Y. L. Chen, H.-H. Chu, J. G. Analytis, Z. K. Liu, K. Igarashi, H.-H. Kuo, X. L. Qi, S. K. Mo, R. G. Moore, D. H. Lu, M. Hashimoto, T. Sasagawa, S. C. Zhang, I. R. Fisher, Z. Hussain, and Z. X. Shen, Massive Dirac Fermion on the Surface of a Magnetically Doped Topological Insulator, *Science* **329**, 659 (2010)
- <sup>24</sup>P. Loš'ák, Č. Drašar, I. Klichová, J. Navrátil, T. Černohorský, Properties of Bi<sub>2</sub>Se<sub>3</sub> Single Crystals Doped with Fe Atoms, *physica status solidi (b)*, **200**(1): 289–296 (1997)
- <sup>24</sup>T. C. Farrar and E. D. Becker, *Pulse and Fourier Transform NMR, Introduction to Theory and Methods*, Academic Press, New York, 1971.
- <sup>25</sup>P. A. Beckmann and C. Dybowski, *J. Magn. Res.* **146** (2010) 379-380.
- <sup>26</sup>R. K. Harris, E. D. Becker, S. M.C. De Menezes, R. Goodfellow and P. Granger, *Pure Appl. Chem.* **73** (2001) 1795-1818.
- <sup>27</sup>G. R. Hyde, H. A. Beale, and I. L. Spain, J.A. Woollam, *J. Phys. Chem. Solids* **35** (1974) 1719-1728.
- <sup>28</sup>J. P. Yesinowski, *Top. Curr. Chem.* **306** (2012), 229 – 312.
- <sup>29</sup>W. G. Proctor and F. C. Yu, *Phys. Rev.* **77** (1950), 717.
- <sup>30</sup>W. C. Dickenson, *Phys. Rev.* **77** (1950), 736-737.
- <sup>31</sup>W. D. Knight, *Phys. Rev.* **76** (1949), 1259 -1260.
- <sup>32</sup>M. F. Olekseeva, E. I. Slinko, K. D. Tovstyuk, and A. G. Handozhko, *Phys. Stat. Sol. (A)* **21** (1974), 759 – 762.
- <sup>33</sup>J. Y. Leloup, B. Sapoval and G. Martinez, *Phys. Rev. B* **7** (1973), 5276 – 5284.
- <sup>34</sup>E. R. Andrew, A. Bradbury, and R. G. Eades, *Nature* **182** (1958) 1659.
- <sup>35</sup>E. R. Andrew, A. Bradbury, and R. G. Eades, *Nature* **183** (1959) 1802-1803.
- <sup>36</sup>I. J. Lowe, *Phys. Rev. Lett.* **2** (1959) 285-287.
- <sup>37</sup>M. E. Stoll, R. W. Vaughan, R. B. Saillant, and T. Cole, *J. Chem. Phys.* **61** (1974) 2896-2899.
- <sup>38</sup>S. J. Opella, M. H. Frey, and T. A. Cross, *J. Am. Chem. Soc.* **101** (1979) 5856-5857.
- <sup>39</sup>I. Orion, J. Rocha, S. Jobic, V. Abadie, R. Brec, C. Fernandez, and J-P. Amoureux, *J. Chem. Soc. Dalton Trans.* **20** (1997), 3741–3748.

- <sup>40</sup>N. Zumbulyadis, P. M. Henrichs, and R. H. Young, *J. Chem. Phys.* **75** (1981) 1603-1611.
- <sup>41</sup>A. C. Olivieri, *J. Magn. Reson.* **81** (1989) 201-205.
- <sup>42</sup>D. L. Bryce and G. D. Sward, *Magn. Reson. Chem.* **44** (2006) 409-450.
- <sup>43</sup>R. E. Taylor, S. Bai, and C. Dybowski, *J. Mol. Struct.* **987** (2011) 193-198.
- <sup>44</sup>J. Herzfeld and A. E. Berger, *J. Chem. Phys.* **73** (1980) 6021-6030.
- <sup>45</sup>Y. Y. Hu and K. Schmidt-Rohr, *Solid State NMR* **40** (2011) 51–59.
- <sup>46</sup>M. Deschamps, C. Roiland, B. Bureau, G. Yang, L. LePollès, and D. Massiot, *Solid State NMR* **40** (2011) 72–77.
- <sup>47</sup>A. Abragam, *Principles of Nuclear Magnetism*, Oxford University Press, Oxford, 1961, pp, 196 and 392.
- <sup>48</sup>B. Sutter, R. E. Taylor, L. R. Hossner, and D. W. Ming, *Soil Sci. Soc. Am. J.* **66** (2002) 455-463.
- <sup>49</sup>R. E. Taylor, Fahri Alkan, C. Dybowski, and Louis-S. Bouchard, lead telluride (in preparation).
- <sup>50</sup>F. H. Larsen, H. J. Jakobsen, P. D. Ellis, and N. C. Nielsen, *J. Phys. Chem. A* **101** (1997) 8597-8606.
- <sup>51</sup>R. Siegel, T. T. Nakashima, and R. E. Wasylshen, *J. Phys. Chem. B* **108** (2004) 2218-2226.
- <sup>52</sup>I. Hung, A. J. Rossini, and R. W. Schurko, *J. Phys. Chem. A* **108** (2004) 7112-7120.
- <sup>53</sup>S.K. Mishra, S. Satpathy, and O. Jepsen, *J. Phys.: Condens. Matter* **9** (1997) 461-470.